JARQ 43 (3), 227 – 237 (2009) http://www.jircas.affrc.go.jp

Ventilation Design for a Chick Incubator Using Computational Fluid Dynamics

In-bok LEE[1], Sadanori SASE[2]*, Hwa-taek HAN[3], Hi-ki HONG[4], Si-heung SUNG[5], Hyun-sub HWANG[1], Se-woon HONG[1], Il-hwan SEO[1] and Soon-Hong KWON[6]

[1] Department of Rural Systems Engineering, Seoul National University (Seoul 151–742, Korea)
[2] Department of Rural Technologies, National Institute for Rural Engineering, National Agriculture and Food Research Organization (Tsukuba, Ibaraki 305–8609, Japan)
[3] School of Mechanical and Automotive Engineering, Kook Min University (Seoul 136–702, Korea)
[4] School of Mechanical and Industrial System Engineering, Kyung Hee University (Seoul 136–702, Korea)
[5] Department of Biosystems Engineering, Konkuk University (Chungju 380–701, Korea)
[6] College of Natural Resource and Life Sciences, Pusan National University (Pusan 609–735, Korea)

Abstract

We used aerodynamic technology to develop a ventilation system for a prototype chick incubator. We used computational fluid dynamics (CFD) to analyze the internal airflow and distribution of air within the incubator. We used local mean age (LMA) and local mean residual time (LMR) theory to examine the accuracy of the CFD model and to quantify the ventilation efficiency. The largest CFD error was only –3.5%, proving the reliability of the model for studying the ventilation efficiency of the incubator. We also compared the total mass flow rates of the inlet and outlet slots and examined the mass balance of the CFD model. The comparison showed an error of –0.8% at a ventilation rate of 100% and –1.2% at 50%. The CFD results show that the ventilation system improved the ventilation efficiency of the chick incubator. The incoming fresh air was evenly supplied to all cages via a duct and a diffuser installed in the central passageway, and contaminated air was exhausted through the outlet system before being diffused to the cages. The sizes of the inlet and outlet slots were very important in improving the uniformity of ventilation. The angle of the diffuser installed in the ceiling inlet was also critically important in maintaining a uniform air pressure and airflow at the inlet slots.

Discipline: Agricultural facilities
Additional key words: local mean age, local mean residual time

Introduction

Various efforts and studies to improve the raising conditions of animals have been carried out. However, ventilation studies are limited because of the difficulty in analyzing airflow, which is invisible and unpredictable[1,3,8]. To solve this problem, many recent studies have used aerodynamic technology to study and improve the ventilation systems of livestock houses[11,12,13,14].

The biggest difficulty with existing poultry houses is uniformity of conditions. In Korea, most of the cage-type poultry houses with typical forced ventilation systems generally have the inlets on a side wall and the outlets on the ceiling; the inlets on a side wall and outlets on the other side wall; or tunnel-type ventilation[15]. In these systems, the stability, suitability, and uniformity of conditions are not satisfied, and ventilation efficiency is thus very low.

As of December 2005, Korea had a total of 101 693 000 poultry, about 47% of which were broilers[16]. Since 2001, the number of growers raising 30 000 to 50 000 and more than 50 000 broilers had increased by 28% and 70%, respectively. This increase in production has increased the recognition of the importance of optimally controlling the environment in poultry farming.

*Corresponding author: e-mail sase@affrc.go.jp
Received 5 November 2007; accepted 27 November 2008.

However, a verified ventilation system suitable for all four seasons in Korea has not yet been developed. Moreover, most of the current ventilation system models are imported from Europe, where conditions are different.

Generally, chicks hatch in a hatchery and are transferred within a day to broiler houses, where they are raised until sold. However, chicks show high mortality in the broiler house during the first 7 days. Suitable environmental conditions and proper ventilation in the broiler house during this critical stage are very important. Moreover, improving the raising conditions then would greatly decrease mortality and illness of the chicks and thus produce healthier poultry[17,21].

The ultimate goal of the study was to find an optimum ventilation system for a transportable chick incubator. The ventilation system aimed to uniformly deliver fresh air to all cages of the incubator and discharge contaminants before they are diffused to the chicks. Because a field experiment requires enormous cost, time, and effort to find the optimum system, an aerodynamic simulation using computational fluid dynamics (CFD) was conducted. CFD uses numerical methods and algorithms to solve and analyze problems that involve fluid and air flow. This computer-based method is faster and more economical than other methods, and allows the structure of the cages and environmental factors to be manipulated in various ways. However, the accuracy of the CFD technique must be tested initially, as the designer's skill and knowledge of the technology can significantly influence the results. After an optimum model was found using the CFD technology, a chick incubator was built following the CFD results, and the data collected in the incubator were used to verify the CFD model.

Materials and methods

1. Experimental facilities

(1) Incubator design

The chick incubator framework design presented in Fig. 1 has 12 cages arranged in two columns and six rows. The cage height was set at 200 mm with conveyor belts placed 200 mm below each cage for manure manage-

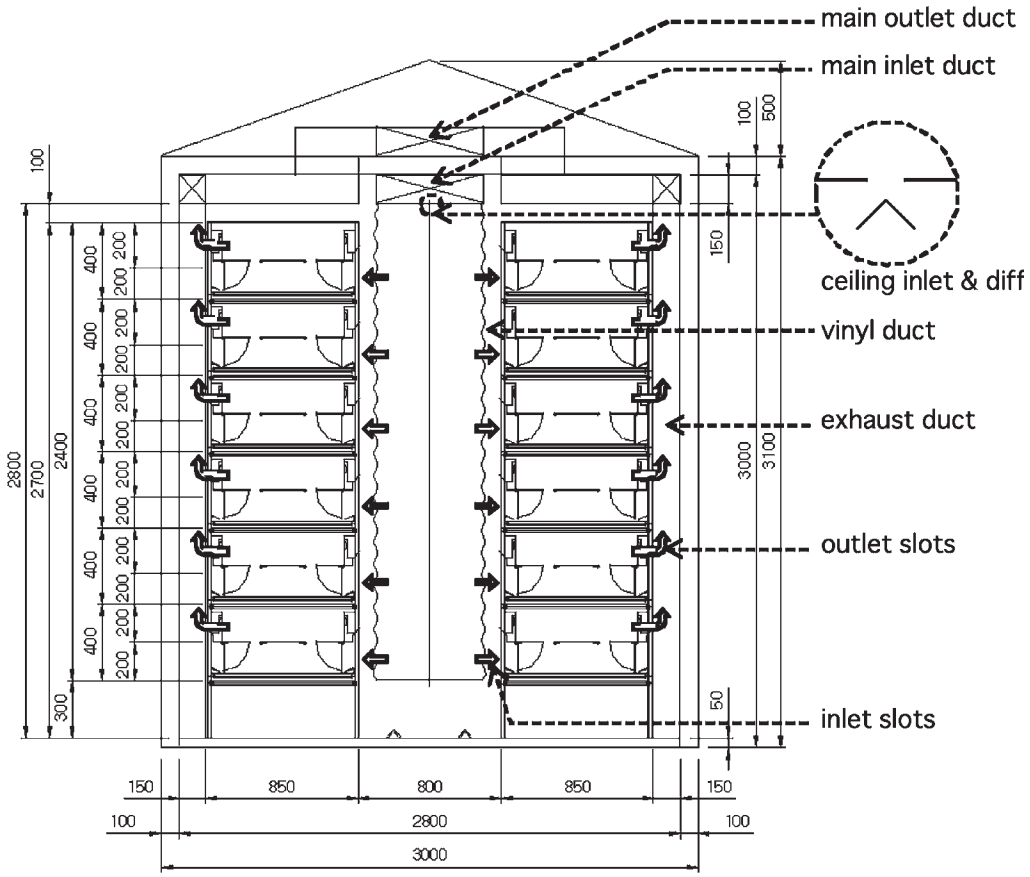

Fig. 1. End view of a chick incubator model (units, mm)
The ceiling inlet opening and the diffuser just below it are shown in cross-section.

ment. The widths of each cage and the passageway were set to 850 and 800 mm, respectively. A hard PVC duct to deliver fresh air to all cages was installed in the central passageway of the incubator. The duct is unfolded most of the time during the ventilation period and can be folded away for access. The ventilating inlet slots located at both sides of the PCV duct were installed at equal height just below the cages to avoid blowing air on chicks.

A temperature and humidity control system was installed where the main inlet and outlet ducts were connected to maintain an optimum air temperature around the chicks and to maintain an optimum energy balance, especially during the cold season. The outlet slots were located at equal height on both side walls to lead to the main vertical exhaust duct.

The most important consideration in determining the size of an incubator is conformity to the Korean Road and Transportation Law[9], which specifies that it should be transportable on roads. The dimensions of the chick incubator were set at 11.15 m (L) × 3.0 m (W) × 3.6 m (H). Approximately 10 000 chicks can be raised at one time in the incubator for 7 days. The prototype chick incubator is shown in Fig. 2.

(2) Computational fluid dynamics

The CFD programs used in the study were STAR-CD version 4.10 (CD-Adapco, Melville, NY, USA) and Fluent CFD version 6.2 (Fluent Co., Lebanon, NH, USA). The accuracy of the CFD model was tested by using LMA/LMR theory and mass balance. LMA refers to the time it takes for air to travel from an inlet to a given point inside, and LMR to the time it takes for air to travel from a given point inside to an outlet. Mass (1), momentum (2), and energy (3) conservation equations[4,5,10] were also used in the CFD application and analysis:

$$\frac{\partial \rho}{\partial t} + \nabla \cdot (\rho \vec{v}) = S_m \tag{1}$$

$$\frac{\partial}{\partial t}(\rho \vec{v}) + \nabla \cdot (\rho \vec{v} \vec{v}) = -\nabla P + \nabla \cdot (\bar{\tau}) + \rho \vec{g} + \vec{F} \tag{2}$$

$$\frac{\partial}{\partial t}(\rho E) + \nabla \cdot (\vec{v}(\rho E + P)) = \nabla \cdot (k_{eff} \nabla T - \sum_j h_j \vec{J}_j + (\bar{\tau}_{eff} \vec{v})) + S_h \tag{3}$$

where E = total energy (kJ s^{-1}), $\vec{F}$ = external body force (N m^{-3}), $\vec{g}$ = gravity acceleration (m s^{-2}), h_j = specific enthalpy of species j (J kg^{-1}), $\vec{J}_j$ = diffusion flux of species j (kg m^{-2} s^{-1}), k_{eff} = effective conductivity (W m^{-1} K^{-1}), P = pressure (Pa), S_h = total entropy (J K^{-1}), S_m = mass source (kg m^{-3} s^{-1}), T = temperature (K), $\vec{v}$ = velocity (m s^{-1}), ρ = density (kg m^{-3}), τ = stress tensor (Pa), and $\bar{\tau}_{eff}$ = effective stress tensor (Pa).

(3) Ventilation efficiency analysis

We analyzed the ventilation efficiency by an LMA/LMR function connected to the CFD main module through a user defined function[7,19]. The application of LMA/LMR analysis was thoroughly explained by Sandberg et al.[18] and Han et al.[7], and the importance of ventilation efficiency analysis was discussed in detail by Han[6] and Sandberg[19]. The ventilation efficiency was determined from the air exchange rate at each internal location (24 in total) and the uniformity in the feeding environment inside. Even if two identical interior spaces have equal ventilation rates, the ventilation efficiency varies according to the location of the ventilation inlets and outlets. Since livestock houses constantly generate dusts, gases, and other contaminants, it is not reliable to depend only on the overall ventilation rate, especially in ventilation system design.

There are three methods for finding the LMA and LMR by experiment: step-up, step-down, and pulse. We

Fig. 2. A prototype of the chick incubator

used the step-down method. A total of 24 measuring points were designated for measuring LMA and LMR: in each cage and at the conveyor belts. The ideal in ventilation efficiency is to get complete mixing with an even distribution of gas concentration. In a complete mixing state, the ventilation rate per hour, Q ($m^3\ h^{-1}$), within an interior volume V (m^3) gives the air exchange rate (h^{-1}) or ventilation rate. The inverse of the ventilation rate is time, called the nominal time constant (τ_n):

$$\tau_n = \frac{V}{Q} \tag{4}$$

If LMR >> τ_n, the local exhaust index (ε_p) is low. Likewise, if LMA << τ_n, the local supply index (α_p) is low. These indexes represent the ventilation efficiency at a given point inside. Since LMR at an inlet is the time it takes for a contaminant to travel from the inlet to an outlet, it is therefore equal to the LMA at an outlet. The analysis therefore considers the assumption that the LMA at an outlet (LMA_{ex}) = the LMR at an inlet (LMR_{sup}). Theoretically, it is also equal to τ_n[6,7,18,19]:

$$\tau_n = LMA_{ex} = LMR_{\text{sup}} \tag{5}$$

The average local exhaust index of an interior space is defined as the room-mean exhaust effectiveness. It has been shown that the room-mean exhaust efficiency is equal to the room-mean supply efficiency, or the average local supply index of the interior space (Han, 1999; Han et al., 2001). Therefore, the room-mean exhaust efficiency and the room-mean supply efficiency can both be defined as the room-mean ventilation efficiency. In the case of complete interior mixing, the room-mean ventilation efficiency is 50%; and in the case of displacement ventilation, the room-mean ventilation efficiency is 100%. In Eq. (6), <ε> represents a mean value:

$$< \varepsilon >= \frac{\tau_n}{2 \cdot < LMR >} = \frac{\tau_n}{2 \cdot < LMA >} \tag{6}$$

We used a tracer gas decay method using carbon dioxide (CO_2). In the step-down method, the CO_2 concentration of the inlet air and of the internal volume was 400 ppm. To measure LMA, we generated 2000 ppm CO_2 as tracer gas at the inlet and then measured concentrations at all 24 points inside. To measure LMR at a given point, we released the tracer gas there and measured the concentration at the outlet. Equations (7) and (8) show LMA and LMR, respectively, for a point p. The overall LMA and LMR of the internal space are shown in Eq. (9). The superscripts and subscripts indicate the location of the tracer gas injection and its measuring spot, respectively.

$$LMA_p = \frac{\int_0^\infty t^2 \cdot C_p^{sup}(t)dt}{\int_0^\infty C_p^{sup}(t)dt} \tag{7}$$

$$LMR_p = \frac{\int_0^\infty t^2 \cdot C_{ex}^{p}(t)dt}{\int_0^\infty C_{ex}^{p}(t)dt} \tag{8}$$

$$< LMA >=< LMR >= \frac{\int_0^\infty t^2 \cdot C_{ex}^{sup}(t)dt}{\int_0^\infty C_{ex}^{sup}(t)dt} \tag{9}$$

where LMA = local mean age (s), LMR = local mean residual time (s), t = time (s), C = gas concentration (ppm), p = an internal point, ex = location of outlet, and sup = location of inlet.

Each outlet and inlet in the CFD model had 15 cells, and since each cell has different velocities and gas concentrations, the weighted mean at the vent opening of the model was used to calculate the LMA and LMR in Eq. (10):

$$LMA, LMR = \frac{\sum_{i=1}^{n}\left(C_i \times V_i \times A_i\right)}{V \times A} \tag{10}$$

where A = total area of vent opening (m^2), A_i = area of cells i (m^2), C_i = gas concentration (mass fraction), n = total number of cells, V = velocity at vent opening ($m\ s^{-1}$), and V_i = velocity at cell i ($m\ s^{-1}$).

2. Experimental procedures

Designing a chick incubator in an accurate 3D CFD model more cells than a Pentium IV processor can handle. Therefore, we used a 2D CFD model with 100 400 hexahedral cells. The effect of screen type, feeding line, and water supply were not included in the model as their influence on airflow is very small and insignificant. Chicks were also neglected, since the purpose of the simulation was to find an optimum ventilation system, and it is difficult to design a 3D distribution of chicks in a 2D simulation model. However, the model considered the belts designed to manage chick manure, as they can exert a great influence on the internal airflow. The left half of a symmetrical incubator was incorporated into the CFD model, and the boundary wall along the passageway was made into a symmetric wall for effective meshing. This reduced the number of squares in the mesh and the computer operating time.

We also used a 2D CFD model to design the optimum ventilation system, to design the inlet and outlet ducts and their best locations. All surface temperatures were set at 27°C. The kinetic energy (Eq. (11)) and dissipation rate (Eq. (12)) at the inlet were specified as follows:

$$k = \frac{3}{2}(v \cdot I)^2 \tag{11}$$

$$\varepsilon = C_{\mu}^{3/4} \frac{k^{3/2}}{\gamma} \tag{12}$$

where k = turbulent kinetic energy ($m^2\ s^{-2}$), v = air velocity ($m\ s^{-1}$), I = turbulent intensity (%), ε = turbulent dissipation rate ($m^2\ s^{-3}$), C_{μ}, = empirical constant (0.09), and γ = turbulence length scale (m).

Turbulent models are a key factor in enhancing the accuracy of CFD simulations. We used the RNG (renormalization group) κ–ε model (Eqs. (13) and (14)). Several reports proved the reliability and accuracy of the model in analyzing various flow problems in agricultural facilities[14].

$$\rho \frac{Dk}{Dt} = \frac{\partial}{\partial x_i}\left[\left(\mu + \frac{\mu_t}{\sigma_k}\right)\frac{\partial k}{\partial x_i}\right] + G_k + G_b - \rho\varepsilon - Y_M \tag{13}$$

$$\rho \frac{D\varepsilon}{Dt} = \frac{\partial}{\partial x_i}\left[\left(\mu + \frac{\mu_t}{\sigma_\varepsilon}\right)\frac{\partial \varepsilon}{\partial x_i}\right] + C_{1\varepsilon}\frac{\varepsilon}{k}(G_k + C_{3\varepsilon}G_b) - C_{2\varepsilon}\rho\frac{\varepsilon^2}{k} \tag{14}$$

where $C_{1\varepsilon}$ = constant (1.44), $C_{2\varepsilon}$ = constant (1.92), t = time (s), ρ = density ($kg\ m^{-3}$), k = turbulent kinetic energy ($m^2\ s^{-2}$), ε = turbulent dissipation rate ($m^2\ s^{-3}$), μ_t = turbulent viscosity (m^2 s), G_k = generation of turbulent kinetic energy due to mean velocity gradients ($kg\ m^{-1}\ s^{-2}$), G_b = generation of kinetic energy due to buoyancy ($kg\ m^{-1}\ s^{-2}$), Y_M = contribution of fluctuating dilatation in compressible turbulence to the overall dissipation rate ($kg\ m^{-1}\ s^{-2}$), σ_k = turbulent Prandtl number for k (1.0), and σ_ε = turbulent Prandtl number for ε (1.3).

First, we had to carefully consider the optimum ventilation design before we could find a detailed structural design by CFD. The main consideration was to improve the uniformity, stability, and suitability of internal environmental factors, typically air temperature in this study.

The main structural factors intended to improve the internal environmental conditions were vertically installed inlet and exhaust ducts (Fig. 1). We assumed that they improve the uniformity of environmental conditions in all cages. We also assumed that the internal volume to be environmentally controlled can be decreased and that the thermal resistance of the side walls can be improved. We also examined the effect of the diffuser installed at the ceiling inlet at maintaining the uniformity of air pressure at the inlet slots of the vertically installed PVC inlet duct. The sizes of the inlet and outlet slots are also important factors in achieving uniformity of mass flow rates at the slots.

In the preliminary model, the sizes of both inlets and outlets were set to 5 cm, and the width of the vertical exhaust pipe was set to 10 cm. Each of these sizes should be carefully decided to uniformly deliver fresh air to all cages of the incubator and to discharge contaminants before they are diffused to the chicks. Accordingly, the ventilation efficiencies with the various inlet and outlet sizes were examined by using the time-dependent computed 2D CFD models while the LMA/LMR function was connected to the CFD main module to be computed simultaneously in order to analyze the ventilation efficiency. The CFD environmental factors are shown in Table 1. We used two methods to test the validity and accuracy of the CFD models in order to check the reliability of the CFD-computed results. First, the total mass flow rates at the inlet and outlet slots were compared to examine the mass balance of the CFD model. Second, the errors of the CFD results were examined by Eqs. (4) and (5) under the assumption that LMA_{ex} = LMR_{sup} (= τ_n)[6,7,18,19] (Eq. (5)).

Results and discussion

1. Optimum ventilation design

Equation (15) of Bruce[2] and Wathes & Charles[20] was

Table 1. Constant input values for the CFD model

Contents	Value	Unit
Design air temperature	300.15	K
Design relative humidity	70.0	%
Wall surface temperature	300.15	K
Cage surface temperature	300.15	K
Floor surface temperature	300.15	K
Density of internal air	1.147	$kg\ m^{-3}$
Viscosity of internal air	1.83E-05	$kg\ m^{-1}\ s^{-1}$
Thermal conductivity of internal air	0.0262	$W\ m^{-1}\ K^{-1}$
Specific heat of internal air	1004.0	$J\ kg^{-1}\ K^{-1}$
Mass diffusivity of internal air	1.56E-05	$m^2\ s^{-1}$
Molecular weight of internal air	28.966	$g\ mol^{-1}$
Gravitational acceleration of internal air	9.81	$m\ s^{-2}$
Atmospheric pressure	101.325	kPa

used to calculate maximum ventilation rate, giving 62.7 $m^3\ h^{-1}$. This value was then used in the CFD analysis as 100% ventilation rate, and 31.4 $m^3\ h^{-1}$ was used as 50% ventilation rate:

$$\text{Maximum ventilation rate } 1.5\times10^{-3} m^3 s^{-1} kg^{0.75} \qquad (15)$$

Many problems emerged during the CFD analysis. First, the greatest volume of airflow was seen at the bottom-most inlet slot of the vinyl duct, because the downward incoming air from the central ceiling inlet generated high pressure at the bottom. Thus, it was impossible to evenly deliver fresh air to each cage. Moreover, the greatest volume of air was exhausted through the topmost outlet slots. It was therefore necessary to resize the outlet slots at each cage, increasing from the smallest at the top to the largest at the bottom. This exhausted an even volume of air at each height. The CFD simulation was again run and the results were analyzed and compared. Although there would be many experimental cases for the slot sizes, we decided to make the size of the inlets on the vinyl duct equal and use only the diffuser at the ceiling inlet to generate equal pressure at each inlet. Then each outlet slot was appropriately sized.

The inlet slots on both sides of the vinyl duct were uniformly set to 3 cm, and a diffuser on the ceiling inlet was installed to generate uniform air pressure at every incoming slot. The goal was to maintain a consistent pressure vertically along the vinyl duct. The CFD analysis determined the appropriate angle of the diffuser to be 70° to 75°. The preliminary CFD analysis results showed that the air volumes were equalized at most of the outlet slots when the outlets measured 5, 6, 8, 10, 12, and 12 cm from top to bottom and the diameter of the vertical exhaust pipe was 15 cm.

The CFD model was run in the final design in three cases (Fig. 3): case 1, without a diffuser or vinyl duct; case 2, without a vinyl duct but with a diffuser; and case 3, with a vinyl duct and a diffuser. The angle of the diffuser was set at 70° for cases 2 and 3. Figures 3 and 4 show the CFD airflow distributions in the incubator when the ventilation rate was 100% and 50%, respectively. In case 1, most of the incoming air from the ceiling inlet passed through the central passageway and diffused early before reaching the bottom cage. This resulted in a lower volumetric flow rate at the lower outlet slots than at the upper outlet slots. In case 2, incoming fresh air was supplied only to the upper cages and the fresh air outlets immediately at the main outlet. This showed that the diffuser was not helpful in delivering the incoming fresh air to all the cages. Case 3 gave a good result, with a nearly uniform distribution of fresh air to the cages. This revealed that the combination of the diffuser and vinyl duct was very helpful in uniformly supplying fresh air to all the cages.

Tables 2 and 3 show the air velocities and mass flow

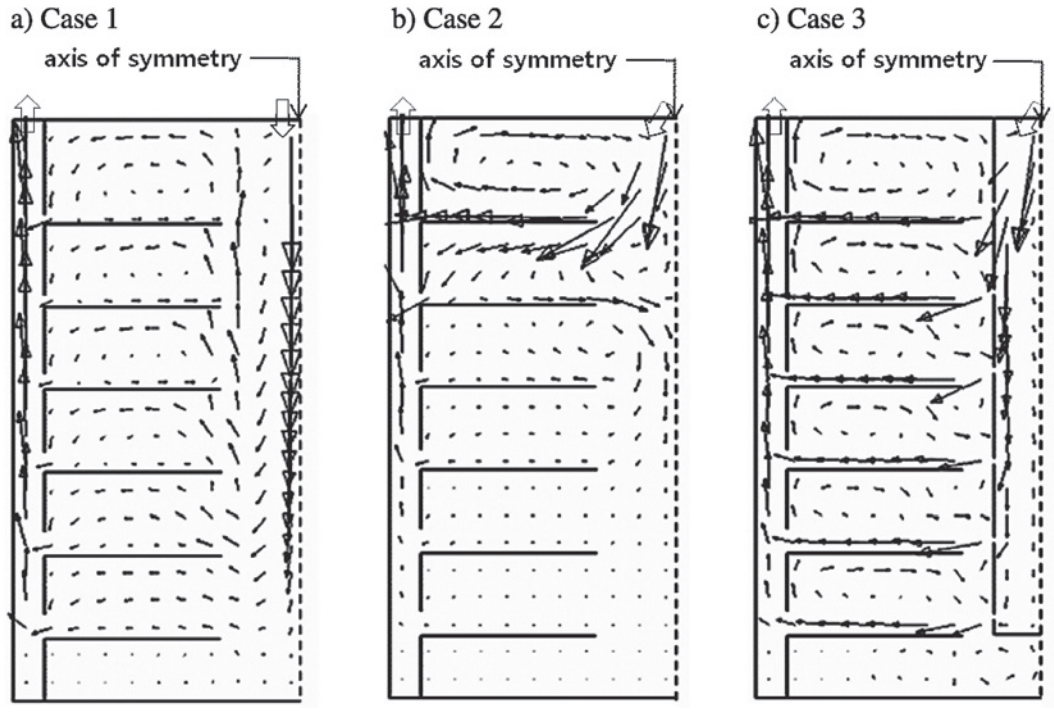

Fig. 3. Airflow pattern at 100% ventilation rate with a maximum air velocity of 1.576 m s^{-1}

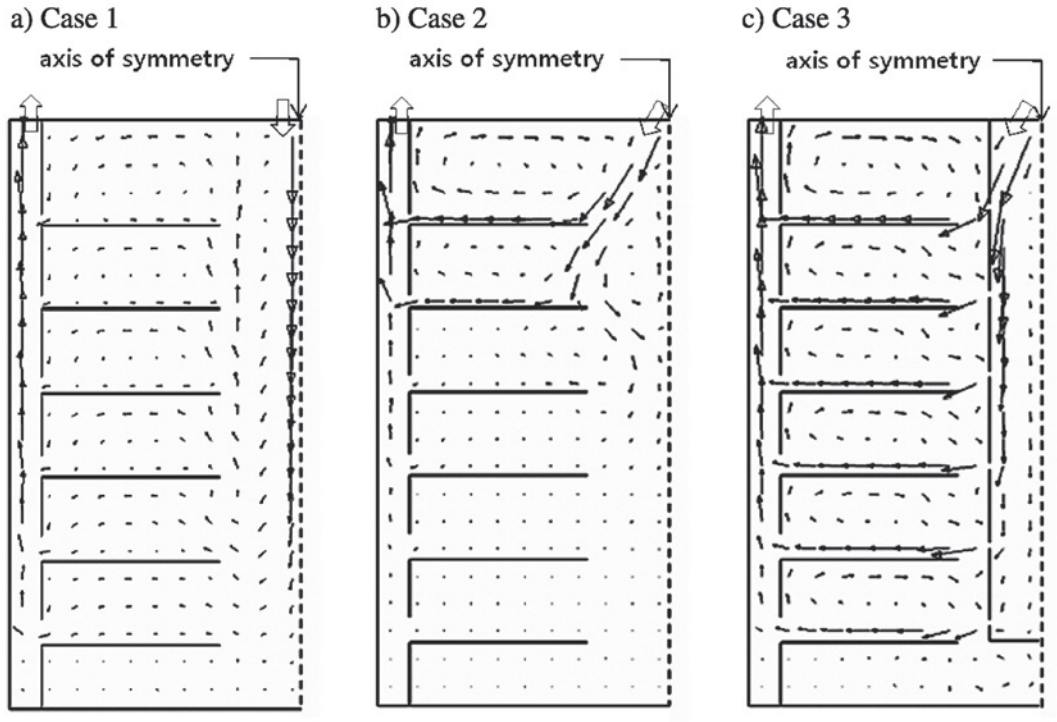

Fig. 4. Airflow pattern at 50% ventilation rate with a maximum air velocity of 0.862 m s^{-1}

Table 2. Air velocity and mass flow rate from bottom to top in case 3 at 100% ventilation rate

Inlet	Width (m)	*U* (m s^{-1})	Mass flow rate (kg s^{-1})	Outlet	Width (m)	*U* (m s^{-1})	Mass flow rate (kg s^{-1})
1	0.03	0.88	0.0312	1	0.12	0.17	0.0240
2	0.03	0.82	0.0291	2	0.12	0.24	0.0333
3	0.03	0.78	0.0276	3	0.10	0.22	0.0256
4	0.03	0.73	0.0259	4	0.08	0.29	0.0269
5	0.03	0.78	0.0277	5	0.06	0.33	0.0230
6	0.03	0.95	0.0337	6	0.05	0.67	0.0393
Total			0.1752				0.1721

Table 3. Air velocity and mass flow rate from bottom to top in case 3 at 50% ventilation rate

Inlet	Width (m)	*U* (m s^{-1})	Mass flow rate (kg s^{-1})	Outlet	Width (m^2)	*U* (m s^{-1})	Mass flow rate (kg s^{-1})
1	0.03	0.43	0.0153	1	0.12	0.08	0.0114
2	0.03	0.40	0.0143	2	0.12	0.12	0.0166
3	0.03	0.38	0.0135	3	0.10	0.10	0.0121
4	0.03	0.37	0.0131	4	0.08	0.14	0.0127
5	0.03	0.39	0.0139	5	0.06	0.16	0.0115
6	0.03	0.51	0.0180	6	0.05	0.38	0.0221
Total			0.0881				0.0864

rates at the inlet and outlet slots for case 3 at 100% and 50% ventilation rates. Inlets 1 to 6 are located from bottom to top. The air velocities and mass flow rates at the inlets gave an almost uniform supply of fresh air to all the cages, but a higher value at the bottom inlet slot. This can be explained by the high pressure created at the bottom of the vinyl duct even though a diffuser was installed at the ceiling inlet. The CFD-computed air velocities at the inlet slots appeared to be high enough to stress the chicks, but the air velocities at the chick locations were mostly <0.2 m s^{-1}, which is insufficient to cause stress. High velocities and mass flow rates were also recorded at the bottom outlet, but these can be remedied by making the outlet slot smaller. Comparing the uniformity of the inlet and outlet slots at 100% and 50% ventilation rates showed that the range of the mass flow rate at the outlet was almost twice as large as at the inlet.

2. LMA and LMR investigation

The ventilation efficiencies of the three cases were investigated by using the computed LMA and LMR values. Case 3 with 100% ventilation rate (Fig. 5) showed much more uniform LMA and LMR values than cases 1 and 2. The LMA of case 1 showed that the fresh air from the ceiling inlet rarely reached the upper cages because the air flowed down through the central passageway and then diffused from the bottom to the outlet slots. Very high LMAs were found at the lowest cage in case 2, indicating that fresh air did not reach the lowest cage; the diffuser distributed fresh air only to the upper cages. This agrees with the observed airflow pattern in case 2 at both 100% and 50% ventilation rates. On the other hand, case 3 showed much more uniform LMA at all cages, with maximum values at locations P3 and P4 of the lowest cage. The LMA value at those locations may have been affected by the empty space below the lowest cage. It therefore seems advisable to completely close the space below the lowest cage or to install one more outlet slot there.

The average LMRs at the manure belts were 19.7 s in case 1, 26.0 s in case 2, and 8.5 s in case 3. This shows that gases and dusts at the manure belts were effectively exhausted before being diffused to the chick locations. In this study, the inlet and outlet slots were located next to the manure belts. Locating the inlet and outlet slots just next to the chick locations could further improve the ventilation efficiency.

When the ventilation rate was 50%, the computed LMA and LMR were approximately double those at 100% (Fig. 6). The average LMAs were 21.3 s in case 1, 45.9 s in case 2, and 18.0 s in case 3 at 100% ventilation rate, and 42.6, 95.7, and 35.0 s, respectively, at 50%. The average LMRs were 16.8 s in case 1, 27.7 s in case 2, and 19.1 s in case at 100% ventilation rate, and 34.4, 47.6, and 36.4 s, respectively, at 50%. Compared with case 1, the average LMA of case 3 was much improved by using the vinyl inlet duct installed in the aisle. However, the LMA became much higher if only the vinyl inlet duct was used without the diffuser at the ceiling inlet (case 2). The average LMR in case 3 was comparable with that in case 1 because there were no significant changes in outlet conditions. If we used the inlet slots of the inlet vinyl duct as the inlet point instead of the ceiling inlet, we got much lower LMA and LMR values in case 3 than in case 1. However, unfortunately, we cannot verify this quantitatively because the LMA/LMR theory used in this study can be used with only one inlet and one outlet. For this reason, the LMA uniformity of case 3 was not better than that of case 1. Accordingly, the averaged LMAs at highest and lowest chick locations were 1.5 and 32.9, respectively, even though the inlet slots were located just next to the chick locations to supply fresh air uniformly. The standard deviations of the averaged LMA at the chick locations were 7.3 in case 1, 62.8 in case 2, and 10.5 in case 3 at 100% ventilation rate; the standard deviations of the averaged LMR were 11.2, 22.8, and 5.0, respectively. These results show that the uniformity of the ventilation efficiency was acceptable. The results obtained from each cage at 100% and 50% ventilation rates also showed that the ventilation design with the vinyl duct and diffuser greatly improved the ventilation efficiency of the chick incubator. When the vinyl duct was not installed, case 1 gave better ventilation efficiency than case 2.

3. Examination of CFD accuracy

We used two methods to test the validity and accuracy of the CFD model. First, we compared the total mass flow rates of the inlet and outlet slots to examine the mass balance of the CFD model. As shown in Tables 2 and 3, the total mass flow rates of the inlet and outlet slots were 0.1752 and 0.1721 kg s^{-1}, respectively, at 100% ventilation rate, and 0.0881 and 0.0864 kg s^{-1} at 50%. The widths of the inlet and outlet slots are shown in Tables 2 and 3; the thickness of the 2D CFD model was assumed to be 1 m. The results were almost equal, demonstrating the reliability of the CFD model. Assuming that the inlet mass flow was correct, the errors were –0.8% at 100% ventilation rate and –1.2% at 50%.

Second, the errors of the CFD results were examined by Eqs. (4) and (5) under the assumption mentioned before. The nominal time constant (τ_n) was computed using Eq. (4) with internal dimensions of the incubator of 10.0 m (L) × 2.8 m (W) × 2.8 m (H), which give a total volume of 78.4 m^3:

$$\tau_n = \frac{V}{Q} = \frac{78.4 \quad m^3}{10906.77 \quad m^3 \quad h^{-1}} = 0.007188195 \quad h = 25.88 \quad s$$

The value of τ_n = 25.88 s should therefore be equal to LMA_{ex} and LMR_{sup}. Comparing the LMA_{ex} and LMR_{sup} results from the CFD analysis, we determined the CFD error (Table 4). The average errors for LMA_{ex} were –0.41% at 100% ventilation rate and –0.55% at 50%. The average errors for LMR_{sup} were –1.35% at 100% ventilation rate and –2.54% at 50%. The largest error was only –2.82% at 100% and only –3.52% at 50%.

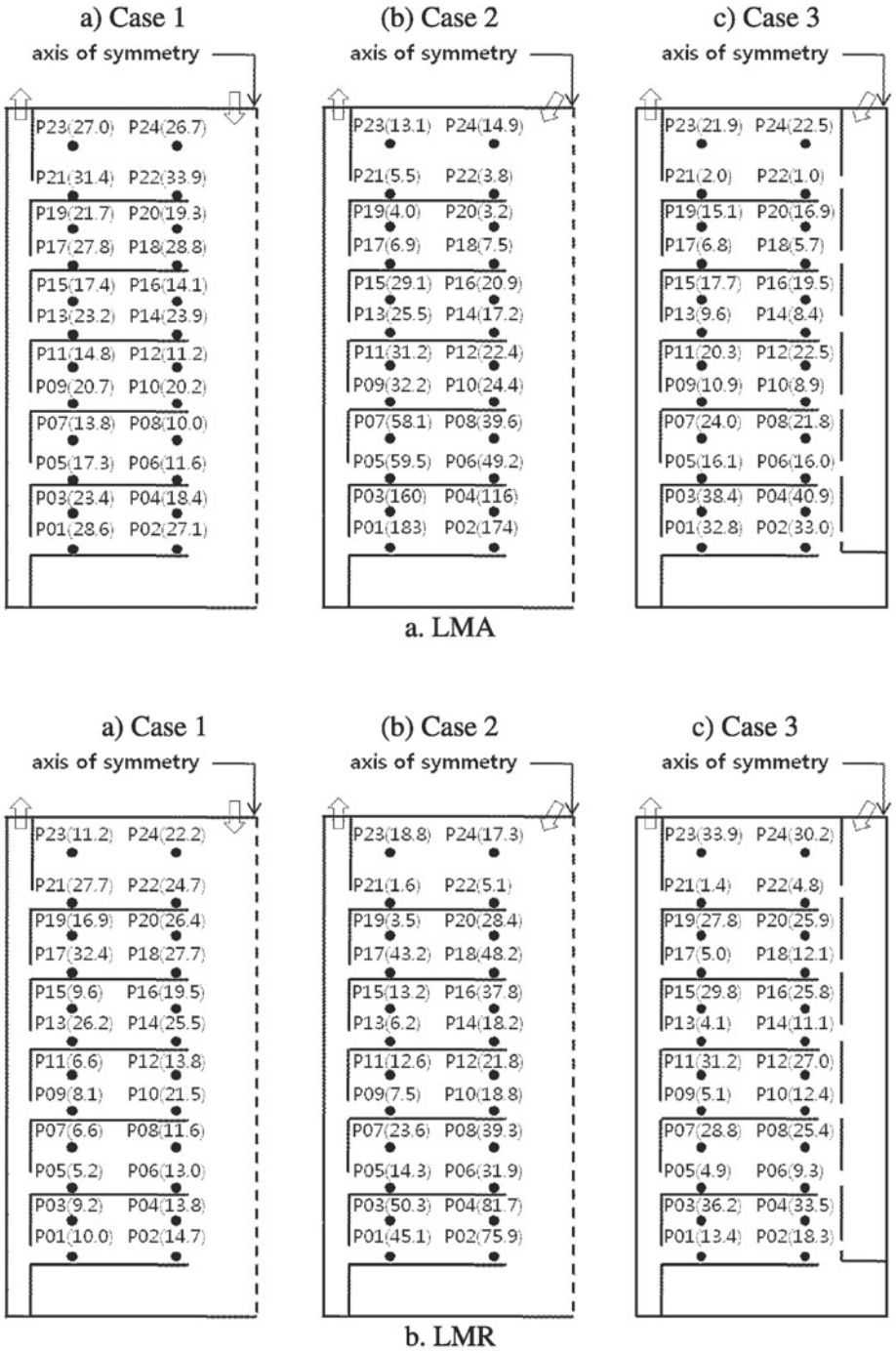

Fig. 5. CFD-computed LMA and LMR values at ventilation rate of 100%

Conclusions

The CFD results show that the ventilation system we designed improved the ventilation efficiency of the chick incubator. The CFD simulation confirmed that the size of each inlet and outlet slot and the width of the main exhaust duct had a major impact on ventilation effectiveness. The incoming fresh air could be evenly supplied to the chick locations by using a diffuser and a vinyl duct with appropriately sized inlet and outlet slots. The angle of the diffuser was also critically important in maintaining a uniform air pressure and airflow at the inlet slots.

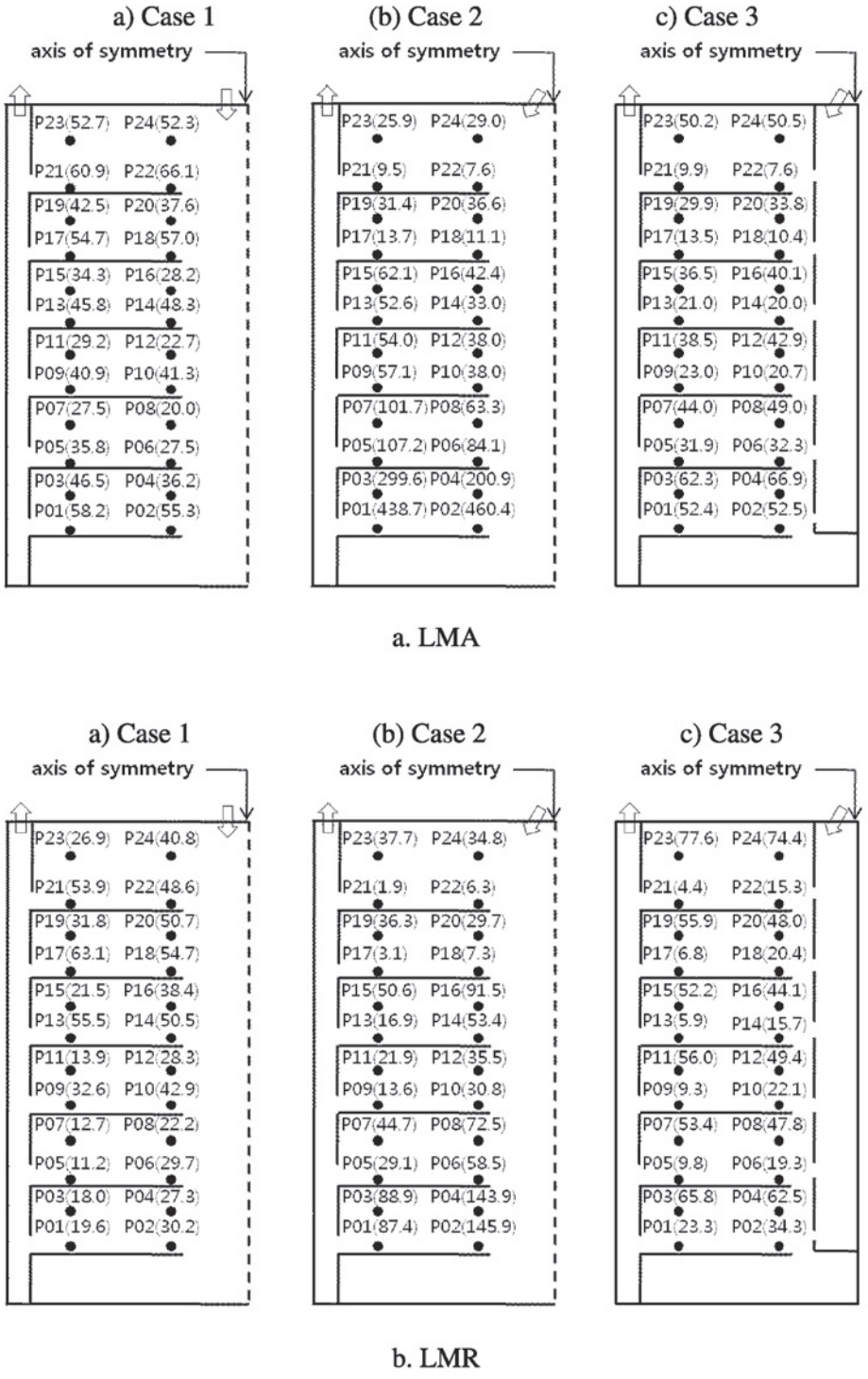

Fig. 6. CFD-computed LMA and LMR values at ventilation rate of 50%

Table 4. Computed LMA_{ex}, LMR_{sup}, and CFD error at 100% and 50% ventilation rates

Case	100% ventilation rate; τ_n = 25.88 s				50% ventilation rate; τ_n = 51.76 s			
	LMA_{ex} (s)	Error (%)	LMR_{sup} (s)	Error (%)	LMA_{ex} (s)	Error (%)	LMR_{sup} (s)	Error (%)
1	25.79	–0.35	25.94	0.23	51.58	–0.35	50.18	–3.05
2	25.79	–0.35	25.15	–2.82	51.26	–0.97	49.94	–3.52
3	25.74	–0.54	25.61	–1.04	51.59	–0.33	52.30	1.04
Average		–0.41		–1.35		–0.55		–2.54

Results of the mass balance of the CFD model at 100% and 50% ventilation rates showed errors of only –0.8% and –1.2%, respectively, confirming the reliability of the model. Moreover, comparisons of CFD results revealed that the largest error of the CFD model was only –3.52% in LMR, further substantiating the accuracy of the model. This proves that the CFD simulation technology is an effective tool for evaluating relative performance and air distribution patterns of alternative designs of livestock houses and structures. Moreover, the LMA/LMR theory proved to be very effective in studying ventilation efficiencies.

Acknowledgments

This paper reports the results obtained in the Korea–Japan joint project on “Structural design and environmental control of large-sized agricultural buildings by latest aerodynamic techniques”.

References

1. Brown-Brandl, T. M. et al. (1997) Temperature humidity index for growing tom turkeys. *Trans. ASAE*, **40**(1), 203–209.
2. Bruce, M. (1981) Ventilation and temperature control criteria for pigs. *In* Environmental Aspects of Housing for Animal Production, ed. Clark, J.A. Butterworths, London, 197–216.
3. Choiniere, Y., Marquis, B. & Gingras, G. (1997) Indoor air quality with and/or without pit ventilation in an early weaning pig barn. Proc. 5th Int. Symp. Livestock Environment, Minnesota, USA, **2**, 866–874.
4. Choudhury, D. (1995) Introduction to the renormalization group method and turbulence modeling. *In* Technical Memorandum TM-107, Fluent Inc., Lebanon, NH, USA.
5. Fluent Inc. (2006) Manual of Computational Fluid Dynamics, version 5.5. Lebanon, NH, USA.
6. Han, H. (1999) Definition of ventilation effectiveness. *Soc. Air Cond. Refrig. Eng. Korea*, **28**(1), 38–47.
7. Han, H., Choi, S. & Jang, K. (2001) Distribution of local supply and exhaust effectiveness according to the room airflow patterns. *Korean J. Air-Cond. Refrig. Eng.*, **13**(9), 853–859.
8. Khankari, K. et al. (1997) Computational analysis of ceiling inlet ventilation systems for livestock buildings. Proc. 5th Int. Symp. Livestock Environment, Minnesota, USA, **1**, 32–39.
9. Korea Transportation Safety Authority (2006) http://www.kotsa.or.kr/collect/laws/la_frm_rule.jsp.
10. Launder, B. E. & Spalding, D. B. (1974) The numerical computation of turbulent flows. *Comput. Meth. Appl. Mech. Eng.*, **3**(2), 269–289.
11. Lee, I. et al. (2002a) Study of livestock housing ventilation by aerodynamic approach. *Proc. Korean Soc. Livest. Hous. Environ.*, 51–58.
12. Lee, I. et al. (2002b) Optimum design of forced ventilation system of piglet house using computer simulation. ASAE Paper No. 024109. St. Joseph, MI, USA.
13. Lee, I. et al. (2003) A study of aerodynamics in agriculture – modern technologies. *CIGR Ejournal*, **5**. http://cigr-ejournal.tamu.edu/.
14. Lee, I., Sase, S. & Sung, S. (2007) Evaluation of CFD accuracy for the study on ventilation of a naturally ventilated broiler house. *JARQ*, **41**, 53–64.
15. Livestock Special Farming (2001) Rural Development Administration, Pub. No. 11-1390000-000948-10, Suwon, Korea.
16. NAPQMS (2006) Statistical survey of livestock industry. National Agricultural Product Quality Management Service, Suwon, Korea.
17. Reece, N. & Lott, B. (1982) Heat and moisture production of broiler chickens during brooding. *Poult. Sci.*, **61**, 661–666.
18 Sandberg, M. & Sjoberg, M. (1983) The use of moments for assessing air quality in ventilated rooms. *Build. Environ.*, **18**(4), 181–197.
19 Sandberg, M. (1992) Ventilation effectiveness and purging flow rate-A review. *In* Proc. Int. Symp. Room Air Convection and Ventilation Effectiveness, Tokyo, Japan, 17–27.
20. Wathes, C. & Charles, D. (1994) Livestock Housing, CAB Int., Wallingford, UK.
21. Xin, H. et al. (1992) Responses of prefasted growing turkeys to acute heat exposure. *Trans. ASAE*, **35**(1), 315–318.